LINEAR STABILITY ANALYSIS FOR SEVERE SLUGGING: SENSITIVITY TO VOID FRACTION CORRELATIONS

G. R. Azevedo [1]**, J. L. Baliño** [2]**, K. P. Burr** [3]

[1,2]Departamento de Engenharia Mecânica, Escola Politécnica, Universidade de São Paulo, São Paulo, Brazil
[3]Centro de Engenharia, Modelagem e Ciências Sociais Aplicadas, Universidade Federal do ABC, Santo André, Brazil

[1]gazevedo00@gmail.com, [2]jlbalino@usp.br, [3]karl.burr@ufabc.edu.br

ABSTRACT

In this paper a numerical linear stability analysis is performed to a mathematical model for the two-phase flow in a pipeline-riser system. Void fraction is a key variable, as it influences the mixture properties and slip between the phases. In the model, it is assumed that an algebraic relationship exists between the void fraction and the state variables. This general representation allows to use empirical or drift flux based correlations. For a correct prediction of the stability behavior of a pipeline-riser flow, preventing the occurrence of severe slugging, it is important to assess the sensitivity of the system response to different void fraction correlations. Three void fraction correlations are implemented: Bendiksen (1984), Chexal et al. (1997) and Bhagwat and Ghajar (2014). The resulting stability maps and state variables profiles for vertical risers are compared for the different correlations. Results show that the different correlations give similar stability maps, with very small differences in the near horizontal branch (low gas superficial velocities) of the stability boundary and slight differences in the near vertical branch (low liquid superficial velocities). The different void fraction correlations show the right experimental trend by increasing the unstable region as the equivalent buffer length in the pipeline is increased.

Keywords: severe slugging, pipeline-riser system, air-water flow, linear stability theory, petroleum production technology

1. INTRODUCTION

Severe slugging may appear in offshore oil production systems for low gas and liquid flow rates when a section with downward inclination angle (pipeline) is followed by another section with an upward inclination (riser). This phenomenon, characterized by the formation and cyclical production of long liquid slugs and fast gas blowdown, may have a period of hours, causing higher average pressures, instantaneous flow rates and oscillations at the reservoir. These operational conditions may lead to the oil production shutdown. The steps leading to the process of severe slugging formation can be seen in Taitel (1986).

Many studies for severe slugging in air-water systems were made, specially for vertical riser with one-dimensional and isothermal flow and a mixture momentum equation in which only the gravitational term is relevant (Taitel et al., 1990; Sarica and Shoham, 1991). In all these models, inertial effects and propagation of pressure waves were neglected, resulting in the no-pressure-wave (NPW) approximation (Masella et al., 1998). As a result of this approximation, pressure changes are felt instantaneously at any point in the riser. Besides, a stratified flow pattern was assumed at the pipeline and variations of void fraction were neglected. The void fraction at the pipeline was obtained from a momentum balance in the gas and liquid phases, resulting in an algebraic relation between the mean variables (Taitel and Dukler, 1976).

In Baliño et al. (2010) a model including friction term and riser variable inclination was presented, while in Baliño (2012, 2014) the model was improved by taking into account inertial effects using the rigid water-hammer approximation.

A pipeline-riser system is designed to operate at steady state. However, it is possible that this condition does not exist. The stability of a pipeline-riser flow depends on the set of parameters that defines the operational state. It is common to represent the stability in a map with liquid and gas reference superficial velocities in the axes, leaving the rest of the parameters fixed. The stability curve is defined as the relationship between the superficial velocities at the stability boundary between the regions where the stationary state is stable or unstable.

Many stability criteria were developed based on simplified models for vertical risers ((Bøe, 1981; Taitel, 1986; Pots et al., 1987; Jansen et al., 1996). Although these stability criteria are useful for a first estimation of the unstable region (they are even used in commercial steady-state computer codes), a common drawback is that they were not derived from complete dynamic system models, but from ad-hoc conditions in which many physical effects were disregarded; consequently, their applicability is quite limited.

The stability curve for any pipeline riser system can be obtained numerically. The stationary solution for a given point in the system parameter space is given as initial condition for the numerical simulation; if the numerical solution does not go away from the initial condition with time, the stationary solution is stable and it is the system steady state. If the numerical solution goes away with time, the stationary state is unstable, there is no steady state and an intermittent solution develops with time. By changing the point and repeating this process, the stability map can be built. For unstable flow, the analysis of the oscillatory solution leads to the determination of the flow regime map, showing the regions correspond-

ing to the different types of intermittency.

As a numerically cost efficient alternative to temporal simulations, the linear stability theory is a powerful technique to identify the stable and unstable regions. To perform the linear stability analysis of a dynamic system, a model characterized by a set of governing equations is needed. Then, the stationary state is obtained by setting to zero the time derivatives. The governing equations are linearized with respect to the stationary solution. These linearized equations determine how infinitesimal perturbations of the stationary solution evolve with time. The growth rate of the perturbations is given by the real part of the eigenvalues of the spectrum associated with the linearized equations. If all eigenvalues have negative real part, then the stationary solution is stable, but if at least one eigenvalue has positive real part, the stationary solution is unstable.

In Zakarian (2000), the linear stability theory was applied for a pipeline-riser system with a vertical riser using the NPW model and considering only two nodes. All dependent variables were considered to vary linearly in space. Then, gas and liquid mass conservation equations and a mixture linear momentum conservation equation were integrated in space. To close the model, an algebraic drift-flux relation was considered resulting in a system of differential-algebraic equations. For a vertical riser, an equation for the flow instability evolution was presented. The stability maps obtained showed a good qualitative agreement with the experimental results reported in the literature.

In Azevedo et al. (2015), a linear stability analysis was made for the model developed in Baliño et al. (2010), considering an arbitrary discretization and including severe slugging mitigation devices such as increase in separation pressure, choke valve at the top of the riser and gas injection at the bottom of the riser. Results were compared with experimental and numerical results reported in the literature with excellent agreement. The results also showed a better agreement with experimental results and with the stability curves obtained through numerical time simulations when the nodalization is increased from the simplest two-node description made in Zakarian (2000).

The void fraction averaged on the flow passage area is a key variable in the behavior of multiphase systems, as it affects virtually all the mixture variables and transport processes. The determination of the void fraction is usually made through correlations in which it is assumed that the void fraction depends algebraically on the process variables. Moreover, many void fraction correlations are framed in the drift flux model (Zuber and Findlay, 1965; Wallis, 1969), in which attention is focused on the relative motion rather than on the motion of the individual phases.

As many multiphase models and commercial computer codes are based on the void fraction behavior, it is important to study the sensitivity of the system response to the drift flux correlation. In this paper, the influence of different drift flux correlations on the stability of a mul-

tiphase model is studied. Three correlations are studied: Bendiksen (1984), Chexal et al. (1997) and Bhagwat and Ghajar (2014).

A comparison is made for the stationary state and for the stability maps. The results obtained show that the drift flux correlation alters the stationary state and influences the stability maps for the boundaries corresponding to higher gas superficial velocities.

2. MODEL

The model equations are based on Baliño et al. (2010). It considers one-dimensional flow in both pipeline and riser subsystems. The liquid phase is assumed incompressible, while the gas phase is considered as an ideal gas. The two-phase flow is in isothermal condition and the flow pattern, in the pipeline, is assumed as a stratified flow. At the separator, a constant pressure is assumed. In this paper, no additional severe slugging mitigation devices are considered.

2.1 Pipeline

As stated in Baliño et al. (2010), the pipeline can be either in a condition of liquid accumulation or in a condition of continuous gas penetration (see Fig. 1). As the stationary state exists only for the condition of continuous gas penetration ($x = 0$), the equations for the pipeline subsystem can be written as:
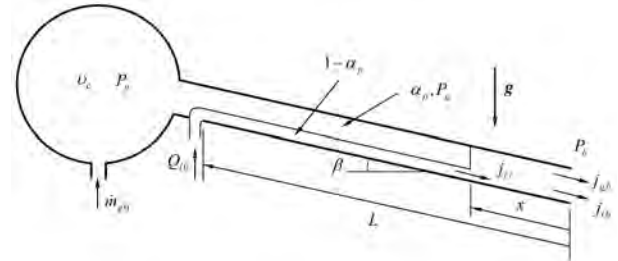

Figure 1: Definition of variables at the pipeline (from Baliño et al. (2010)).

$$j_{lb} = j_{l0} \tag{1}$$

$$\frac{dP_b}{dt} = \frac{-P_b\, j_{gb} + \frac{T_g}{T_0}\, P_0\, j_{g0}}{L\, \alpha_p + L_e} \tag{2}$$

where j_{lb} and j_{gb} are, respectively, the superficial velocities for the liquid and gas at the bottom of the riser, L is the pipeline length, P_b and P_g are, respectively, the pressure at the bottom of the riser and the gas pressure ($P_b = P_g$), T_g is the gas temperature, t is time and α_p and β are respectively the pipeline void fraction and inclination angle (positive when downwards). The superficial velocities at a reference condition for gas and liquid, respectively j_{g0} and j_{l0}, used to represent the stability maps, are defined as:

$$j_{g0} = \frac{R_g\, T_0\, \dot{m}_{g0}}{P_0\, A} \tag{3}$$

$$j_{l0} = \frac{Q_{l0}}{A} \tag{4}$$

where $\dot{m}_{g0}$ is the gas mass flow rate injected in the pipeline, R_g is the gas constant and Q_{l0} is the liquid volumetric flow injected in the pipeline. The reference condition is defined for pressure $P_0 = 1.013 \times 10^5\,Pa$ and temperature $T_0 = 293\,K$.

The existence of a buffer vessel with volume v_e is considered in order to simulate an equivalent pipeline length $L_e = \frac{v_e}{A}$, where A is the flow passage area ($A = \frac{1}{4}\pi D^2$, where D is the inner diameter).

As stated before, variations in the pipeline void fraction α_p are neglected during the transient; this assumption is justified, as in Baliño (2012, 2014) it was shown that void fraction variations in the pipeline are very small. The value used in the transients is determined from an algebraic relationship evaluated for the stationary state (Taitel and Dukler, 1976).

2.2 Riser

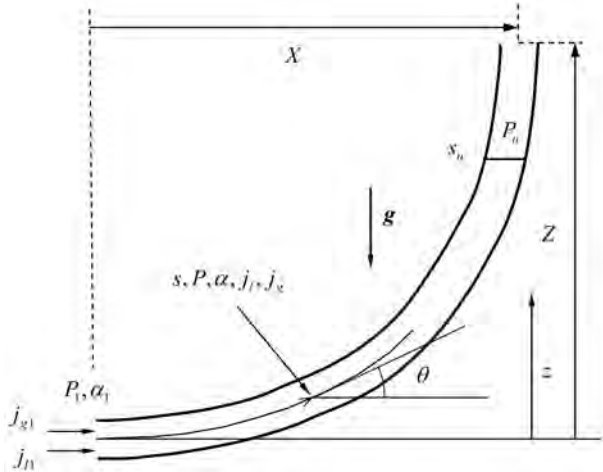Based on Fig. 2, the conservation equations for the riser can be written as:

Figure 2: Definition of variables at the riser (from Baliño *et al.* (2010)).

$$-\frac{\partial \alpha}{\partial t} + \frac{\partial j_l}{\partial s} = 0 \tag{5}$$

$$\frac{\partial}{\partial t}(P\,\alpha) + \frac{\partial}{\partial s}(P\,j_g) = 0 \tag{6}$$

A mixture momentum equation is considered, where the inertial terms are neglected:

$$\frac{\partial P}{\partial s} + \rho_m \left(g\sin\theta + 2\,\frac{f_m}{D}\,j\,|j| \right) = 0 \tag{7}$$

The following relations can be written:

$$\rho_m = \rho_l\,(1-\alpha) + \frac{P}{R_g\,T_g}\,\alpha \tag{8}$$

$$f_m = f\left(Re_m, \frac{\epsilon}{D} \right) \tag{9}$$

$$Re_m = \frac{\rho_m\,D\,|j|}{\mu_m} \tag{10}$$

$$j = j_l + j_g \tag{11}$$

$$\mu_m = \mu_l\,(1-\alpha) + \mu_g\,\alpha \tag{12}$$

where g is the gravity acceleration constant, j_g, j_l and j are respectively the gas, liquid and total superficial velocities, P is the pressure, s is the position along the riser, α is the void fraction, μ_g, μ_l and μ_m are respectively the gas, liquid and mixture dynamic viscosities, ρ_l and ρ_m are respectively the liquid and mixture density and θ is the local inclination angle of the riser. The Fanning friction factor f_m depends on the Reynolds number Re_m and the relative roughness ϵ/D, (where ϵ is the pipe roughness) and is calculated from Chen (1979) using a homogeneous mixture two-phase model.

It will be assumed that there is an algebraic relation between the void fraction and the local flow conditions:

$$\alpha = \alpha\,(j_g, j_l, P, \theta) \tag{13}$$

Equation (13) allows for using many empirical void fraction correlations, as well as correlations based on the drift flux model:

$$\alpha = \frac{j_g}{C_d\,j + U_d} \tag{14}$$

It will be assumed that the drift parameters C_d (distribution parameter) and U_d (drift velocity) depend at most on the local flow conditions and inclination angle $\theta = \theta(s)$, this is, $C_d = C_d(\alpha, j_g, j_l, P, \theta)$ and $U_d = U_d(\alpha, j_g, j_l, P, \theta)$.

2.3 Continuity between the subsystems

Assuming the same flow passage area for the pipeline and riser, the pressure and superficial velocities at the bottom of the riser are continuous:

$$P(0, t) = P_1(t) = P_b(t) \tag{15}$$

$$j_l(0, t) = j_{l1}(t) = j_{lb}(t) \tag{16}$$

$$j_g(0, t) = j_{g1}(t) = j_{gb}(t) \tag{17}$$

Pressure at the top of the riser (position s_t) satisfies:

$$P(s_t, t) = P_s \tag{18}$$

3. STATIONARY STATE

The stationary state is used as the initial condition for the transient simulations and also as the base solution for the linear stability analysis. The stationary state can be obtained by setting to zero the time derivatives in the dynamic equations. Variables at stationary state are denoted with superscript $\tilde{\ }$.

3.1 Pipeline

For the pipeline, Eq. (1) and (2) give:

$$\tilde{j}_{lb} = j_{l0} \tag{19}$$

$$\tilde{j}_{gb} = \frac{T_g}{T_0}\,\frac{P_0}{\tilde{P}_b}\,j_{g0} \tag{20}$$

3.2 Riser

For the riser, Eq. (5) and (6) and the coupling conditions (Eq. (15) and (16)), give:

$$\tilde{j}_l = j_{l0} \tag{21}$$

$$\tilde{j}_g = \frac{T_g}{T_0} \frac{P_0}{\tilde{P}} j_{g0} \tag{22}$$

The void fraction in the riser can be calculated from Eq. (13) or from Eq.(14) as:

$$\tilde{\alpha} = \frac{j_{g0}}{\tilde{C}_d j_{g0} + \left(j_{l0} + \tilde{U}_d\right) \frac{T_0}{T_g} \frac{\tilde{P}}{P_0}} \tag{23}$$

The pressure distribution can be calculated by numerically integrating Eq. (7), as all terms are functions of pressure; and as $\tilde{j} > 0$, the stationary pressure satisfies:

$$\frac{\partial \tilde{P}}{\partial s} = -\tilde{\rho}_m \left(g \sin \theta + 2 \frac{\tilde{f}_m}{D} \tilde{j}^2\right) \tag{24}$$

4. PERTURBATION EQUATIONS

4.1 Pipeline

Variables involved in the pipeline dynamics are written in terms of a stationary and a perturbation contribution:

$$j_{lb}(t) = \tilde{j}_{lb} + \hat{j}_{lb}(t) \tag{25}$$

$$j_{gb}(t) = \tilde{j}_{gb} + \hat{j}_{gb}(t) \tag{26}$$

$$P_b(t) = \tilde{P}_b + \hat{P}_b(t) \tag{27}$$

Taking into account Eq. (19) and (20), the pipeline perturbation equations result:

$$\hat{j}_{lb} = 0 \tag{28}$$

$$\frac{d\hat{P}_b}{dt} + C_{gb} \hat{j}_{gb} + C_{pb} \hat{P}_b = 0 \tag{29}$$

where:

$$C_{gb} = \frac{\tilde{P}_b}{L\alpha_p + L_e} \tag{30}$$

$$C_{pb} = \frac{j_{g0}}{L\alpha_p + L_e} \frac{T_g}{T_0} \frac{P_0}{\tilde{P}_b} \tag{31}$$

4.2 Riser

As there is an algebraic relation between void fraction and the rest of the variables, given by Eq. (13), the void fraction can be eliminated, decreasing the system order. After some algebra, the dynamic equations (5) to (7) can be written as:

$$\{A(\{v\})\} + \underline{B} \left\{\frac{\partial v}{\partial t}\right\} + \underline{C} \left\{\frac{\partial v}{\partial s}\right\} = 0 \tag{32}$$

where:

$$\{v\} = \left\{ \begin{array}{c} j_g \\ j_l \\ P \end{array} \right\} \tag{33}$$

$$\{A\} = \left\{ \begin{array}{c} 0 \\ 0 \\ A_3 \end{array} \right\} \tag{34}$$

$$A_3 = \rho_m \left(g \sin \theta + 2 \frac{f j^2}{D}\right) \tag{35}$$

$$\underline{B} = \left\{ \begin{array}{ccc} B_{11} & B_{12} & B_{13} \\ 0 & 0 & B_{23} \\ 0 & 0 & 0 \end{array} \right\} \tag{36}$$

$$B_{11} = -\frac{\partial \alpha}{\partial j_g} \tag{37}$$

$$B_{12} = -\frac{\partial \alpha}{\partial j_l} \tag{38}$$

$$B_{13} = -\frac{\partial \alpha}{\partial P} \tag{39}$$

$$B_{23} = \alpha \tag{40}$$

$$\underline{C} = \left\{ \begin{array}{ccc} 0 & C_{12} & 0 \\ C_{21} & C_{22} & C_{23} \\ 0 & 0 & C_{33} \end{array} \right\} \tag{41}$$

$$C_{12} = 1 \tag{42}$$

$$C_{21} = C_{22} = P \tag{43}$$

$$C_{23} = j_g \tag{44}$$

$$C_{33} = 1 \tag{45}$$

As usual, variables involved in the riser dynamics are written in terms of a stationary and a perturbation contribution (superscript ˆ):

$$j_g = \tilde{j}_g(s) + \hat{j}_g(s, t) \tag{46}$$

$$j_l = \tilde{j}_l(s) + \hat{j}_l(s, t) \tag{47}$$

$$P = \tilde{P}(s) + \hat{P}(s, t) \tag{48}$$

After some algebra, the differential equations for the perturbations can be written as:

$$\underline{\tilde{A}} \{\hat{v}\} + \underline{\tilde{B}} \left\{\frac{\partial \hat{v}}{\partial t}\right\} + \underline{\tilde{C}} \left\{\frac{\partial \hat{v}}{\partial s}\right\} = 0 \tag{49}$$

where:

$$\{\hat{v}\} = \left\{ \begin{array}{c} \hat{j}_g \\ \hat{j}_l \\ \hat{P} \end{array} \right\} \tag{50}$$

$$\tilde{A}_{ij} = \left(\frac{\partial A_i}{\partial v_j} + \sum_k \frac{\partial C_{ik}}{\partial v_j} \frac{\partial v_k}{\partial s} \right)^{\sim} \qquad (51)$$

$$\underline{A} = \left\{ \begin{array}{ccc} 0 & 0 & 0 \\ A_{21} & 0 & A_{23} \\ A_{31} & A_{32} & A_{33} \end{array} \right\} \qquad (52)$$

$$A_{21} = \frac{\partial \tilde{P}}{\partial s} \qquad (53)$$

$$A_{23} = \frac{\partial \tilde{j}_g}{\partial s} \qquad (54)$$

$$A_{31} = -\frac{1}{\tilde{\rho}_m} \frac{\partial \tilde{\rho}_m}{\partial \tilde{j}_g} \frac{\partial \tilde{P}}{\partial s} + \frac{2}{D} \tilde{\rho}_m \frac{\partial}{\partial \tilde{j}_g} \left(\tilde{f}_m \tilde{j}^2 \right) \qquad (55)$$

$$A_{32} = -\frac{1}{\tilde{\rho}_m} \frac{\partial \tilde{\rho}_m}{\partial \tilde{j}_l} \frac{\partial \tilde{P}}{\partial s} + \frac{2}{D} \tilde{\rho}_m \frac{\partial}{\partial \tilde{j}_l} \left(\tilde{f}_m \tilde{j}^2 \right) \qquad (56)$$

$$A_{33} = -\frac{1}{\tilde{\rho}_m} \frac{\partial \tilde{\rho}_m}{\partial \tilde{P}} \frac{\partial \tilde{P}}{\partial s} + \frac{2}{D} \tilde{\rho}_m \tilde{j}^2 \frac{\partial \tilde{f}_m}{\partial \tilde{P}} \qquad (57)$$

$$\tilde{B}_{ij} = (B_{ij})^{\sim} \qquad (58)$$

$$\tilde{C}_{ij} = (C_{ij})^{\sim} \qquad (59)$$

The superscript $^{\sim}$ indicates an evaluation at the stationary condition.

5. DISCRETIZED PERTURBATION EQUATIONS AND STABILITY ANALYSIS

5.1 Discretized perturbation equations

The riser length is discretized in N nodes and Eq. (49) is integrated in the interval $s_i \leq s \leq s_{i+1}$. Representative values for any function ϕ within the integration interval are calculated as:

$$\phi(\tilde{v}) = \phi_{i+1/2} \simeq \frac{1}{2} \left[\phi(\tilde{v}_i) + \phi(\tilde{v}_{i+1}) \right] \qquad (60)$$

Representative values of the perturbed variables, as well as space and time derivatives are calculated as:

$$\hat{v}_{i+1/2} \simeq \frac{1}{2} (\hat{v}_i + \hat{v}_{i+1}) \qquad (61)$$

$$\left(\frac{\partial \hat{v}}{\partial s} \right) = \left(\frac{\partial \hat{v}}{\partial s} \right)_{i+1/2} \simeq \frac{\hat{v}_{i+1} - \hat{v}_i}{\Delta s_i} \qquad (62)$$

$$\left(\frac{\partial \hat{v}}{\partial t} \right) = \left(\frac{\partial \hat{v}}{\partial t} \right)_{i+1/2} \simeq \frac{1}{2} \left(\frac{d\hat{v}_i}{dt} + \frac{d\hat{v}_{i+1}}{dt} \right) \qquad (63)$$

where $\Delta s_i = s_{i+1} - s_i$. The following set of equations is obtained:

$$\underline{G} \left\{ \frac{d\hat{v}}{dt} \right\} + \underline{H} \{\hat{v}\} = 0 \qquad (64)$$

$$\underline{G} = \left[\begin{array}{ccc} G_{11} & G_{12} & G_{13} \\ \underline{0} & \underline{0} & G_{23} \\ \underline{0} & \underline{0} & \underline{0} \end{array} \right] \qquad (65)$$

$$\underline{H} = \left[\begin{array}{ccc} \underline{0} & H_{12} & \underline{0} \\ H_{21} & H_{22} & H_{23} \\ H_{31} & H_{32} & H_{33} \end{array} \right] \qquad (66)$$

In Eq. (64), $\underline{G}$ and $\underline{H}$ are rectangular sparse matrices with dimension $3N - 3 \times 3N$, while $\hat{\underline{v}}$ is the vector of nodal values of the perturbed variables ($3N$ components), defined as:

$$\{\hat{\underline{v}}\}_j = \left\{ \begin{array}{lll} \hat{\tilde{j}}_{gj} & \text{for} & 1 \leq j \leq N \\ \hat{\tilde{j}}_{lj-N} & \text{for} & N+1 \leq j \leq 2N \\ \hat{P}_{j-2N} & \text{for} & 2N+1 \leq j \leq 3N \end{array} \right. \qquad (67)$$

The sub-matrices defined in Eq. (65) and (66) are rectangular sparse matrices with dimension $(N-1) \times N$, with the following non-zero elements:

$$\{G_{11}\}_{i,i} = \{G_{11}\}_{i,i+1} = \frac{1}{2} \{B_{11}\}_{i+1/2} \qquad (68)$$

$$\{G_{12}\}_{i,i} = \{G_{12}\}_{i,i+1} = \frac{1}{2} \{B_{12}\}_{i+1/2} \qquad (69)$$

$$\{G_{13}\}_{i,i} = \{G_{13}\}_{i,i+1} = \frac{1}{2} \{B_{13}\}_{i+1/2} \qquad (70)$$

$$\{G_{23}\}_{i,i} = \{G_{23}\}_{i,i+1} = \frac{1}{2} \{B_{23}\}_{i+1/2} \qquad (71)$$

$$\{H_{12}\}_{i,i} = -\{H_{12}\}_{i,i+1} = -\frac{\{C_{12}\}_{i+1/2}}{\Delta s_i} \qquad (72)$$

$$\{H_{21}\}_{i,i} = \frac{1}{2} \{A_{21}\}_{i+1/2} - \frac{\{C_{21}\}_{i+1/2}}{\Delta s_i} \qquad (73)$$

$$\{H_{21}\}_{i,i+1} = \frac{1}{2} \{A_{21}\}_{i+1/2} + \frac{\{C_{21}\}_{i+1/2}}{\Delta s_i} \qquad (74)$$

$$\{H_{22}\}_{i,i} = -\{H_{22}\}_{i,i+1} = \frac{\{C_{22}\}_{i+1/2}}{\Delta s_i} \qquad (75)$$

$$\{H_{23}\}_{i,i} = \frac{1}{2} \{A_{23}\}_{i+1/2} - \frac{\{C_{23}\}_{i+1/2}}{\Delta s_i} \qquad (76)$$

$$\{H_{23}\}_{i,i+1} = \frac{1}{2} \{A_{23}\}_{i+1/2} + \frac{\{C_{23}\}_{i+1/2}}{\Delta s_i} \qquad (77)$$

$$\{H_{31}\}_{i,i} = \{H_{31}\}_{i,i+1} = \frac{1}{2} \{A_{31}\}_{i+1/2} \qquad (78)$$

$$\{H_{32}\}_{i,i} = \{H_{32}\}_{i,i+1} = \frac{1}{2} \{A_{32}\}_{i+1/2} \qquad (79)$$

$$\{H_{33}\}_{i,i} = \frac{1}{2} \{A_{33}\}_{i+1/2} - \frac{\{C_{33}\}_{i+1/2}}{\Delta s_i} \qquad (80)$$

$$\{H_{33}\}_{i,i+1} = \frac{1}{2} \{A_{33}\}_{i+1/2} + \frac{\{C_{33}\}_{i+1/2}}{\Delta s_i} \qquad (81)$$

To close the system of equations, it is necessary to load three additional lines, corresponding to the boundary conditions. Considering Section 2.3 and Eq. (28) and (29) it results:

$$\hat{j}_{l\,1} = 0 \tag{82}$$

$$\frac{d\hat{P}_1}{dt} + C_{g1}\hat{j}_{g\,1} + C_{p1}\hat{P}_1 = 0 \tag{83}$$

where:

$$C_{g1} = \frac{\tilde{P}_1}{L\alpha_p + L_e} \tag{84}$$

$$C_{p1} = \frac{j_{g0}}{L\alpha_p + L_e}\frac{T_g}{T_0}\frac{P_0}{\tilde{P}_1} \tag{85}$$

Considering a constant pressure separator at top of the riser and from Eq. (18), it gives:

$$\hat{P}_N = 0 \tag{86}$$

It results:

$$\underline{G}^* \left\{ \frac{d\hat{v}}{dt} \right\} + \underline{H}^* \{\hat{v}\} = 0 \tag{87}$$

where the square matrices $\underline{G}^*$ and $\underline{H}^*$ (dimension $3\,N \times 3\,N$) are defined as the matrices $\underline{G}$ and $\underline{H}$ augmented with the boundary conditions.

5.2 Stability Analysis

Considering Eq. (87), the following transformation can be written:

$$\{\hat{v}\} = \{\hat{r}\}\exp(\lambda t) \tag{88}$$

where λ is an eigenvalue and $\{\hat{r}\}$ is an eigenvector. From Eq. (87) and (88):

$$(\lambda\underline{G}^* + \underline{H}^*)\{\hat{r}\} = 0 \tag{89}$$

The transformation from Eq. (88) reduced Eq. (87) to a generalized eigenvalue/vector problem. Equation (89) has no trivial solution only when λ satisfies the characteristic polynomial:

$$\det(\lambda\underline{G}^* + \underline{H}^*) = 0 \tag{90}$$

The stability of the stationary state can be decided according to the solution of characteristic polynomial.

5.3 Numerical implementation

For a set of flow, geometry and simulation parameters, the system of equations corresponding to the stationary state were solved and the matrices $\underline{G}^*$ and $\underline{H}^*$ were assembled.

The numerical procedure was implemented using the software MATLAB (Magrab *et al.*, 2005). The subroutine EIGS, which is the ARPACK implementation for Matlab, was used. ARPACK (Lehoucq *et al.*, 1997) is a set of routines, initially developed to solve large scale eigenvalue problems; it is based on an variation of the Arnoldi process called the Implicitly Restarted

Arnoldi/Lanczos Method (IRAM). ARPACK routines are capable of solving large scale symmetric, nonsymmetric, and generalized eigen-problems. They were designed to compute a subset of eigenvalues with user specified features such as those of largest real part or largest magnitude. For every request, a set of numerically accurate eigenvalues and eigenvectors is available .

In Burr *et al.* (2013) a fixed grid was considered in the plane of superficial velocities, determining the stability for each grid point. In the present work, a routine was implemented to track the stability curve, starting from a point located in the upper branch (low gas superficial velocity and high liquid superficial velocity) and using the bisection method to determine, with the required precision, the neutral stability condition.

6. VOID FRACTION CORRELATIONS

6.1 Bendiksen (1984)

Bendiksen (1984) made experiments in straight tubes with inclination angles between -30° and 90° using air and water in order to measure the velocity of long bubbles. The resulting drift flux correlation is:

$$C_d = \begin{cases} 1.05 + 0.15\sin\theta & \text{for } Fr_j < 3.5 \\ 1.2 & \text{for } Fr_j \geq 3.5 \end{cases} \tag{91}$$

$$U_d = \begin{cases} \sqrt{g\,D}\,(0.35\sin\theta + 0.54\cos\theta) & \text{for } Fr_j < 3.5 \\ 0.35\sqrt{g\,D}\sin\theta & \text{for } Fr_j \geq 3.5 \end{cases} \tag{92}$$

where the Froude number Fr_j is defined as:

$$Fr_j = \frac{j}{\sqrt{g\,D}} \tag{93}$$

Bendiksen's correlation was used in previous contributions (Baliño *et al.*, 2010; Azevedo *et al.*, 2015) because of its simplicity (void fraction is explicit and drift parameters are independent of state variables). The main disadvantage is that the database used is only for low pressure air-water flow and for a restricted flow pattern.

6.2 Chexal *et al.* (1997)

Chexal-Lellouche's correlation (Chexal *et al.*, 1997) covers a full range of conditions and flow orientations, as well as different fluid types (steam-water, air-water and refrigerants), making it suitable for high-pressure systems like the ones in nuclear systems and possibly in petroleum systems; for this reason, it was implemented in codes for large system thermal-hydraulic analysis. The drift parameters satisfy continuity and have finite first derivatives and restrict the resulting void fraction to be in the range from zero to one. Moreover, the drift parameters satisfy limiting conditions for critical and zero pressure, as well as for zero and unity void fraction. Void fraction has to be determined iteratively, as the drift parameters are dependent on the state variables. The resulting drift flux correlation is, for co-current upward air-water flows:

$$C_d = \frac{L}{K_0 + (1 - K_0)\,\alpha^r} \quad (94)$$

where:

$$L = F_r\,L_v + (1 - F_r)\,L_h \quad (95)$$

$$F_r = \left(\frac{\theta}{90^o}\right)^{0.2} \quad (96)$$

$$L_v = \min\left(1.15\alpha^{0.45},\, 1\right) \quad (97)$$

$$L_h = \min\left(1.125\,\alpha^{0.6},\, 1\right)\left[1 + \alpha^{0.05}\,(1 - \alpha)^2\right] \quad (98)$$

$$K_0 = B_1 + (1 - B_1)\left(\frac{\rho_g}{\rho_l}\right)^{0.25} \quad (99)$$

$$r = \frac{1 + 1.57\left(\dfrac{\rho_g}{\rho_l}\right)}{1 - B_1} \quad (100)$$

$$B_1 = F_r\,B_{1v} + (1 - F_r)\,B_{1h} \quad (101)$$

$$B_{1(v,h)} = \min(0.8,\, A_{1(v,h)}) \quad (102)$$

$$A_{1(v,h)} = \frac{1}{1 + \exp\left(-Re_{v,h}/60000\right)} \quad (103)$$

$$Re_v = \begin{cases} Re_g & \text{for } Re_g > Re_l \\ Re_l & \text{for } Re_g < Re_l \end{cases} \quad (104)$$

$$Re_h = \begin{cases} |Re_g| & \text{for } |Re_g| > |Re_l| \\ |Re_l| & \text{for } |Re_g| < |Re_l| \end{cases} \quad (105)$$

$$U_d = 1.41\left[\frac{(\rho_l - \rho_g)\,\sigma\,g}{\rho_l^2}\right]^{0.25} C_1\,C_2\,C_3\,C_4 \quad (106)$$

where σ is the surface tension and:

$$C_1 = (1 - \alpha)^{B_1} \quad (107)$$

$$\text{For } (\rho_l/\rho_g) \le 18 : C_2 = 0.4757\left[\ln\left(\frac{\rho_l}{\rho_g}\right)\right]^{0.7} \quad (108)$$

$$\text{For } (\rho_f/\rho_g) > 18 : \begin{cases} \text{if } C_5 \ge 1, & C_2 = 1 \\ \text{if } C_5 < 1, & C_2 = 1 - \exp\left(\frac{-C_5}{1 - C_5}\right) \end{cases} \quad (109)$$

$$C_5 = \sqrt{\frac{150}{(\rho_l/\rho_g)}} \quad (110)$$

$$C_3 = F_r\,C_{3v} + (1 - F_r)\,C_{3h} \quad (111)$$

$$C_{3v} = \max\left[0.5,\, 2\exp\left(-Re_l/300000\right)\right] \quad (112)$$

$$C_{3h} = \max\left(0.125,\, 0.5\exp\left(-Re_l/300000\right)\right) \quad (113)$$

$$C_4 = \begin{cases} 1 & \text{for } C_7 \ge 1 \\ \dfrac{1}{1 - \exp\left(\dfrac{C_7}{1 - C_7}\right)} & \text{for } C_7 < 1 \end{cases} \quad (114)$$

$$C_7 = \left(\frac{0.09144\,m}{D}\right)^{0.6} \quad (115)$$

6.3 Bhagwat and Ghajar (2014)

Bhagwat and Ghajar (2014) recently presented new equations for the drift parameters applicable to gas-liquid flows in a wide range of fluid combinations, thermodynamic states and pipe diameters, correlating 8255 data points from 60 different sources. For low pressures and air-water flows, this correlation is applicable to different flow patterns and gives similar results as Bendiksen's correlation. The correlation is also implicit in void fraction.

$$C_d = \frac{2 - (\rho_g/\rho_l)^2}{1 + (Re_{tp}/1000)^2} + \frac{\left[\dfrac{1 + (\rho_g/\rho_l)^2 \cos\theta}{1 + \cos\theta}\right]^{\frac{1}{5}(1-\alpha)} + C_{d,1}}{1 + (1000/Re_{tp})^2} \quad (116)$$

where:

$$C_{d,1} = 0.2\left(1 - \sqrt{\frac{\rho_g}{\rho_l}}\right)\left[(2.6 - \beta)^{0.15} - \sqrt{f_{tp}}\right](1 - x)^{1.5} \quad (117)$$

$$\frac{1}{\sqrt{f_{tp}}} = -4\log_{10}\left(\frac{\epsilon/D_h}{3.7} + \frac{1.256}{Re_{tp}\sqrt{f_{tp}}}\right) \quad (118)$$

$$Re_{tp} = \frac{\rho_l\,j\,D}{\mu_l} \quad (119)$$

$$x = \frac{\rho_g\,j_g}{\rho_g\,j_g + \rho_l\,j_l} \quad (120)$$

$$\beta = \frac{j_g}{j_g + j_l} \quad (121)$$

$$U_d = (0.35\sin\theta + 0.45\cos\theta) \times \sqrt{\frac{g\,D\,(\rho_l - \rho_g)}{\rho_l}}\,(1 - \alpha)^{0.5}\,C_2\,C_3\,C_4 \quad (122)$$

where:

$$C_2 = \begin{cases} \left(\dfrac{0.434}{\log_{10}\mu_l^*}\right)^{0.15} & \text{for } \mu_l^* > 10 \\ 1 & \text{for } \mu_l^* \le 10 \end{cases} \quad (123)$$

$$\mu_l^* = \mu_l/(0.001\,Pa\,s) \quad (124)$$

$$C_3 = \begin{cases} (La/0.025)^{0.9} & \text{for } La < 0.025 \\ 1 & \text{for } La \ge 0.025 \end{cases} \quad (125)$$

$$C_4 = \begin{cases} -1 & \text{for } (-50^o \le \theta < 0^o \text{ and } Fr_{sg} \le 0.1) \\ 1 & \text{otherwise} \end{cases} \quad (126)$$

where Fr_{sg} and La are respectively the Froude and Laplace numbers, defined as:

$$Fr_{sg} = \sqrt{\frac{\rho_g}{\rho_l - \rho_g}}\,\frac{j_g}{\sqrt{g\,D\,\cos\theta}} \quad (127)$$

$$La = \frac{\sqrt{\dfrac{\sigma}{g\,(\rho_l - \rho_g)}}}{D} \quad (128)$$

7. RESULTS

Comparative results are shown for the stability maps and the stationary distributions of the state variables for the system conditions from Taitel *et al.* (1990) (see Table 1), corresponding to a vertical riser connected to a separator.

Table 1: Parameters for vertical riser (Taitel *et al.*, 1990).

Definition	Parameter	Value	Unit
Liquid viscosity	μ_l	1×10^{-3}	$kg/(m\,s)$
Gas viscosity	μ_g	1.8×10^{-5}	$kg/(m\,s)$
Liquid density	ρ_l	1000	kg/m^3
Gas constant	R_g	287	$m^2/(s^2\,K)$
Temperature	T_g	293	K
Pipeline length	L	9.1	m
Buffer length	L_e	$1.69, 5.1, 10$	m
Pipeline diameter	D	2.54×10^{-2}	m
Pipeline-riser roughness	ϵ	1.5×10^{-6}	m
Pipeline inclination	β	5	degree
Riser height	Z	3	m
Separator pressure	P_s	1.03×10^5	Pa

In Azevedo *et al.* (2015) discretization and eigenvalues well-posedness studies were made, resulting that $N = 50$ is a satisfactory nodalization.

Figure 3 shows the stability map for a buffer length $L_e = 1.69\,m$ calculated with the linear stability theory, for the different void fraction correlations. It can be observed that the three correlations predict similar stability maps. The differences for the near horizontal branch with low gas superficial velocities are small, because the predicted void fractions are very small for this flow range. For the nearly vertical branch with low liquid superficial velocities, there are slight differences in the predicted stability boundaries.
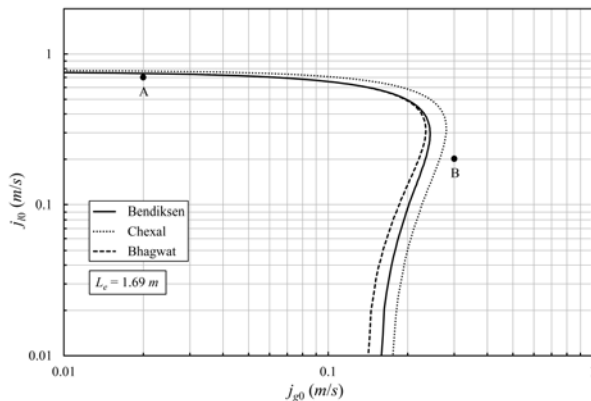

Figure 3: Stability maps for $L_e = 1.69\,m$.

To elucidate the behavior of the different correlations, two operating points were chosen in Fig. 3: point A, corresponding to $j_{g0} = 0.02\,m/s$, $j_{l0} = 0.7\,m/s$, is located closed to the low gas superficial velocity branch, while point B, corresponding to $j_{g0} = 0.3\,m/s$, $j_{l0} = 0.2\,m/s$, is located closed to the high gas superficial velocity branch. Notice that point A is located within the unstable region for any void fraction correlation, so the model predicts that there is no steady state for this configuration; on the other hand, point B is in the stable region.

Figures 4, 5 and 6 show respectively the stationary state profiles in the riser for void fraction, gas superficial velocity and pressure for point A. It can be observed that the void fractions are very low and that Bendiksen's and Bhagwat's correlations give very similar results, while Chexal's correlation gives little higher values. According to the stationary conditions (Eqs. (22) and (23)) as the void fraction is higher, pressure is lower and gas superficial velocity is higher.
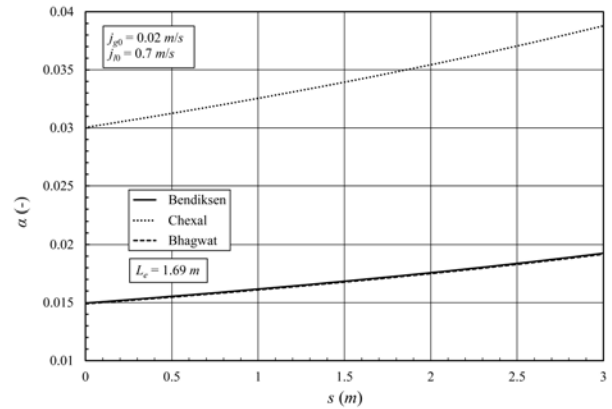

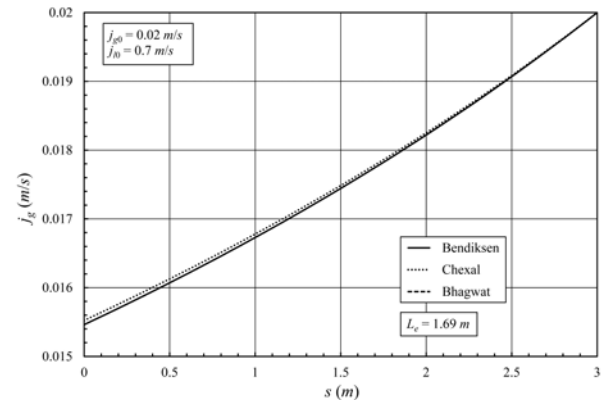Figure 4: Void fraction profile for $L_e = 1.69\,m$ (point A).

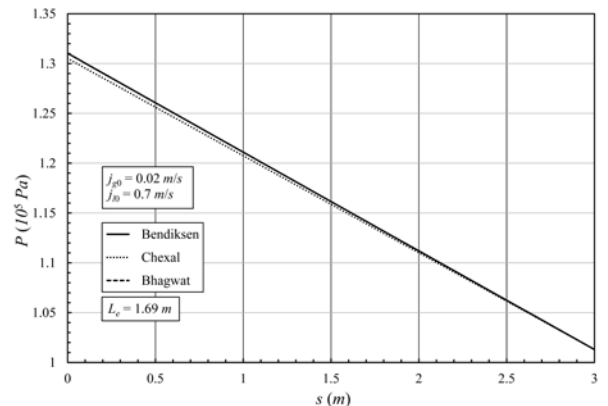Figure 5: Gas superficial velocity profile for $L_e = 1.69\,m$ (point A).

Figure 6: Pressure profile for $L_e = 1.69\,m$ (point A).

Figures 7, 8 and 9 show respectively the stationary

state profiles in the riser for point B. Void fractions are higher; the highest values are predicted by Bhagwat's correlation, followed by Chexal's and Bendiksen's correlations.
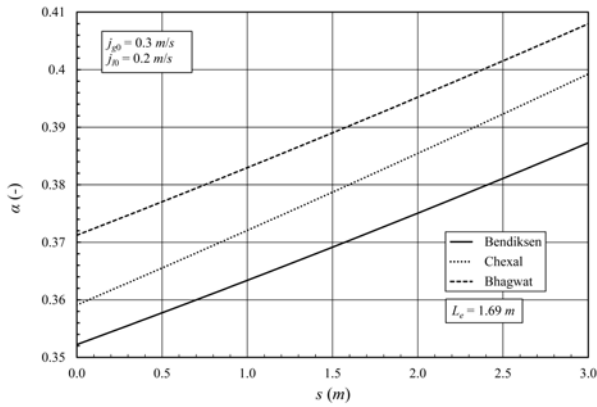

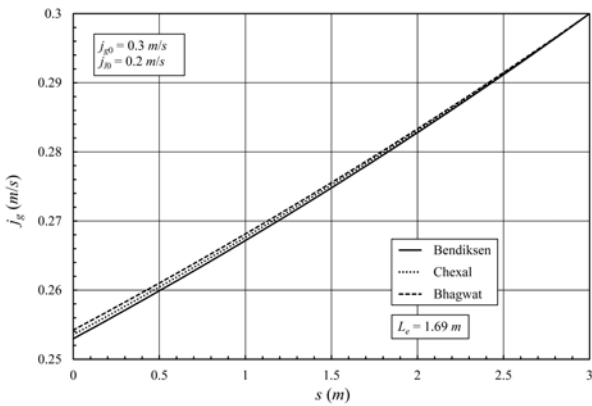Figure 7: Void fraction profile for $L_e = 1.69\,m$ (point B).

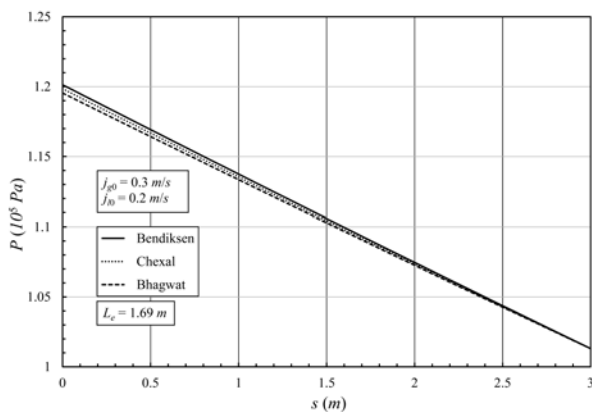Figure 8: Gas superficial velocity profile for $L_e = 1.69\,m$ (point B).

Figure 9: Pressure profile for $L_e = 1.69\,m$ (point B).

Finally, Fig. 10 shows the stability map for a buffer length $L_e = 5.1\,m$ calculated with the linear stability theory, for the different void fraction correlations. It can be observed that the three correlations predict similar stability maps and also an increase in the unstable region for higher buffer lengths, which is in agreement with the experimental trends.
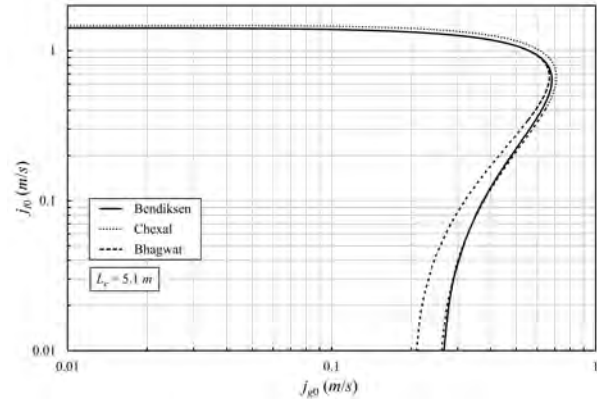

Figure 10: Stability maps for $L_e = 5.1\,m$.

8. CONCLUSIONS

The stability analysis using the linear stability theory was proven to be a very efficient tool to predict the influence of different operating conditions on the occurrence of severe slugging. In particular, three different void fraction correlations were implemented and their influence was assessed. It was found that there is a very small influence on the near horizontal branch of the stability boundary and a slight influence in the near vertical branch. Moreover, the different correlations exhibit the right trend, increasing the unstable region as the buffer equivalent length is increased. Although the correlations give slightly different values of void fraction, the calculations show that the methodology is robust when different correlations are considered.

It would be desirable to extend this methodology for more complex geometries like the ones in hilly terrain flows. For doing this, it is necessary to count with reliable void fraction correlations valid for different pipe inclinations, flow directions and fluid conditions.

As severe slugging is an important issue in the design of offshore petroleum systems, the necessity of including a stability analysis derived from the dynamic models in computer simulation codes is evident; for the case of stationary simulation codes the necessity is even more important, as the dynamic simulation is not available and the stationary solution may not physically exist. If the objective is only deciding about the system stability, the stability module would be an useful tool in dynamic simulation codes as well, as computational cost is much less compared to simulations in the time domain.

REFERENCES

Azevedo, G.R., Baliño, J.L. and Burr, K.P., 2015. "Linear stability analysis for severe slugging in air-water systems considering different mitigation mechanisms". *International Journal of Multiphase Flow*, Vol. 73, pp. 238–250.

Baliño, J.L., 2012. "Modeling and simulation of severe slugging in air-water systems including inertial effects". In *The 6th. International Conference on Integrated Modeling and Analysis in Applied COntrol and Automation (IMAACA 2012)*. Wien, Austria, p. 10.

Baliño, J.L., 2014. "Modeling and simulation of severe slugging in air-water systems including inertial effects". *Journal of Computational Science*, Vol. 5, pp. 482–495.

Baliño, J.L., Burr, K.P. and Nemoto, R.H., 2010. "Modeling and simulation of severe slugging in air-water pipeline-riser systems". *International Journal of Multiphase Flow*, Vol. 36, pp. 643–660.

Bendiksen, K.H., 1984. "An experimental investigation of the motion of long bubbles in inclined tubes". *International Journal of Multiphase Flow*, Vol. 10, No. 4, pp. 467–483.

Bhagwat, S.M. and Ghajar, A.J., 2014. "A flow pattern independent drift flux model based void fraction correlation for a wide range of gas-liquid two phase flow". *International Journal of Multiphase Flow*, Vol. 59, pp. 186–205.

Bøe, A., 1981. *Severe slugging characteristics. Part I: Flow regime for severe slugging. Part II: Point model simulation study*. Trondheim, Norway.

Burr, K.P., Baliño, J.L. and Azevedo, G.R., 2013. "Discretization effects on the linear numerical stability analysis of two-phase flows in pipeline-riser systems". In *Proceedings do XXII International Congress of Mechanical Engineering (COBEM 2013)*. Ribeirão Preto, SP, Brazil, p. 12.

Chen, N.H., 1979. "An explicit equation for friction factor in pipe". *Ind. Engng. Chem. Fundam.*, Vol. 18, pp. 296–297.

Chexal, B., Merilo, M., Maulbetsch, J., Horowitz, J., Harrison, J., Westacott, J., Peterson, C., Kastner, W. and Schmidt, H., 1997. *Void Fraction Technology for Design and Analysis*. EPRI, Palo Alto, California, USA.

Jansen, F.E., Shohan, O. and Taitel, Y., 1996. "The elimination of severe slugging - experiments and modeling". *International Journal of Multiphase Flow*, Vol. 22, No. 6, pp. 1055–1072.

Lehoucq, R.B., Sorensen, D.C. and Yang, C., 1997. *ARPACK Usert's Guide: Solution of Large Scale Eigenvalue Problems with Implicit Restarted Arnoldi Methods*. http://www.caam.rice.edu/software/ARPACK/.

Magrab, E.B., Azarm, S., Belachandran, B., Duncan, J.H., Herold, K.H. and Walsh, G.C., 2005. *An Engineer 's Guide to MATLAB*. Pearson Prentice Hall.

Masella, J.M., Tran, Q.H., Ferre, D. and Pauchon, C., 1998. "Transient simulation of two-phase flows in pipes". *International Journal of Multiphase Flow*, Vol. 24, pp. 739–755.

Pots, B.F.M., Bromilow, I.G. and Konijn, M.J.W.F., 1987. "Severe slug flow in offshore flowline/riser systems". *SPE Production Engineering*, pp. 319–324.

Sarica, C. and Shoham, O., 1991. "A simplified transient model for pipeline-riser systems". *Chemical Engineering Science*, Vol. 46, No. 9, pp. 2167–2179.

Taitel, Y., 1986. "Stability of severe slugging". *International Journal of Multiphase Flow*, Vol. 12, No. 2, pp. 203–217.

Taitel, Y. and Dukler, A.E., 1976. "A model for predicting flow regime transitions in horizontal and near horizontal gas-liquid flow". *AIChE Journal*, Vol. 22, No. 1, pp. 47–55.

Taitel, Y., Vierkand, S., Shoham, O. and Brill, J.P., 1990. "Severe slugging in a riser system: experiments and modeling". *International Journal of Multiphase Flow*, Vol. 16, No. 1, pp. 57–68.

Wallis, G.B., 1969. *One-dimensional Two-phase Flow*. McGraw-Hill Book Company, New York.

Zakarian, E., 2000. "Analysis of two-phase flow instabilities in pipe-riser systems". In *2000 ASME Pressure Vessel and Piping Conference*. ASME, Seattle, Washington, USA, pp. 1–9.

Zuber, N. and Findlay, J., 1965. "Average volumetric concentration in two-phase flow system". *Journal of Heat Transfer*, Vol. 87, p. 453.

AUTHOR BIOGRAPHIES

Gabriel Romualdo de Azevedo was born in Joinville, Brazil, in 1986. He graduated in Mechanical Engineering from Polytechnic School, University of São Paulo (2010). He worked for JKK Consulting (2011-2013) in São Paulo, Brazil. Since 2013, he is a PhD student at University of São Paulo. His research interests are fluid dynamics, multiphase flow and hydrodinamic instabilities.

Jorge Luis Baliño was born in Buenos Aires, Argentina in 1959. He graduated in Nuclear Engineering (1983) and made PhD in Nuclear Engineering (1991)from *Instituto Balseiro*, Argentina. He worked for Techint S.A. (1983-1984), *Centro Atómico Bariloche* and *Instituto Balseiro* (1985-2000) in Argentina, *Instituto de Pesquisas Energéticas e Nucleares* (2001-2003) in São Paulo, Brazil. Since 2004 he is Professor at *Universidade de São Paulo*. His research interests are fluid dynamics, heat transfer and multiphase flow.

Karl Peter Burr was born in São Paulo, Brasil in 1964. Received his Bachelor of Science (1988) and his Master of Science (1993) in Ocean Engineering from University of São Paulo, and his PhD (2001) in Ocean engineering from Massachusetts Institute of Technology. He was a post-doctoral fellow at the MIT Ocean Engineering department (2001-2003) and at the Mechanical Engineering Department of *Escola Politécnica* at University of São Paulo (2004-2007). Since 2008 he is Professor at Federal University of ABC. His research interest are hydrodynamic stability, water waves, aerodynamics and multiphase flows.